JOURNAL OF GEOPHYSICAL RESEARCH, VOL. 113, A00B06, doi:10.1029/2008JA013219, 2008

Particle acceleration at coronal mass ejection–driven interplanetary shocks and the Earth's bow shock

M. I. Desai[1] and D. Burgess[2]

Received 28 March 2008; revised 20 June 2008; accepted 4 August 2008; published 31 October 2008.

[1] Particle acceleration in space plasmas, particularly at collisionless shocks, remains a fundamental yet poorly understood problem in space physics. The most important questions that need to be addressed include (1) where are the particles accelerated, (2) what source material is available for acceleration, (3) what mechanisms are responsible for injecting and accelerating the particles, and (4) how are the particle properties modified during their propagation from the acceleration sites to the observation point? Answering these questions will enable further development of the theoretical framework and models that will facilitate quantitative predictions of key properties of the accelerated particles. In this paper, we review recent observations associated with two distinct but widely studied energetic ion populations: (1) solar energetic particles associated with coronal mass ejection–driven interplanetary shocks and (2) energetic ions observed upstream of the Earth's bow shock. We review the common theoretical concepts and physical processes that are believed to be responsible for accelerating particles at these two types of collisionless shocks, emphasizing the commonalities between these distinct structures and their associated particle populations.

Citation: Desai, M. I., and D. Burgess (2008), Particle acceleration at coronal mass ejection–driven interplanetary shocks and the Earth's bow shock, *J. Geophys. Res.*, *113*, A00B06, doi:10.1029/2008JA013219.

1. Introduction

[2] Particle acceleration is a fundamental process that occurs routinely in diverse astrophysical and heliophysical environments, including the solar corona [e.g., *Wang et al.*, 2006], coronal mass ejection (CME)–driven interplanetary (IP) shocks [e.g., *Desai et al.*, 2004], corotating interaction regions and their bounding shocks [e.g., *Mason et al.*, 2008], planetary bow shocks [e.g., *Desai et al.*, 2000], the solar wind termination shock [e.g., *Stone et al.*, 2005], and supernovae shocks [*Jones and Ellison*, 1991]. Although space-borne remote and in situ satellite observations obtained over the last five decades or so have revolutionized our understanding of the basic physics of particle acceleration in space plasmas, particularly at collisionless shocks, many important questions need to be answered before we can develop the theoretical framework and models that will allow quantitative predictions of key properties of the accelerated particles. The basic questions associated with energetic particle populations are (1) where are the particles accelerated, (2) what source material is available for acceleration, (3) what mechanisms are responsible for injecting and accelerating the particles, and (4) how are the particle properties modified during their propagation from the acceleration sites to the observation point?

[3] In this paper, we will address all four of these questions using recent observations associated with two distinct but widely studied energetic ion populations: (1) solar energetic particles (SEPs) associated with CME-driven interplanetary shocks and (2) energetic ions observed upstream of the Earth's bow shock. The nature, formation, and spatial scales of the shocks in these two cases are different: CME-driven IP shocks are large-scale piston-driven shocks that are formed when faster CMEs propagate through the ambient slower solar wind, while the Earth's bow shock is a significantly smaller standing shock formed when the outflowing supersonic solar wind encounters the Earth's magnetosphere. Nonetheless both types of shocks are believed to have several commonalities, including shock structure, heating, dissipation and the manner in which they accelerate particles. This paper compares the common theoretical concepts and the physical processes responsible for accelerating particles at CME-driven IP shocks and the Earth's bow shock. Such cross-fertilization of common concepts and observational features has already enabled us to understand not only the properties and dynamics of CME-driven shocks and the Earth's bow shock and how particles get accelerated by them but also those of the collisionless shocks present in a wide variety of inaccessible astrophysical sites [e.g., *Lee*, 1982, 1983; *Schwartz*, 2006].

2. Solar Energetic Particles

2.1. Overview

[4] Early observations of SEP events extending up to GeV energies were made with ground-based ionization

[1]Southwest Research Institute, San Antonio, Texas, USA.
[2]Astronomy Unit, Queen Mary, University of London, London, UK.

0148-0227/08/2008JA013219$09.00

Table 1. Evolving Paradigm for SEP Events

Property	Impulsive/Flare-Related 1970s–1990s[a]	Impulsive/Flare-Related 1990s to Present[b]	Gradual/CME-Shock-Related 1970s–1990s[a]	Gradual/CME-Shock-Related 90s to Present[b]
Electron/proton ratio	$\sim 10^2 - 10^4$	$\sim 10^2 - 10^4$	~50–100	~50–100
$^3He/^4He$	~1	~0.04–6[c]	~0.0005[h]	~0.0008–0.06[i]
Fe/O	~1	~0.36–2.3[c]	~0.1	~0.0016–0.06[i]
H/He	~10	~10	~100	~100
Q_{Fe}	~20	energy-dependent increase from ~10–20 over ~0.1–1 MeV/nucleon[d]	~14	energy-dependent increase from ~10–20 over ~0.1–100 MeV/nucleon[j]
Seed particles	heated coronal material	heated coronal material	coronal or solar wind material	heated coronal material, flare and CME-shock accelerated material
In situ particle event duration	hours	hours to days[e]	days	days
Longitude cone	<30°	<30°	~180°	~180°
Radio type	III, V(II)	III, V(II)	II, IV	II, IV, III-*l*[k]
X-ray duration	impulsive (~10 min-1 h)	impulsive (~10 min-1 h)	gradual (>1 h)	gradual (>1 h)
Optical/coronagraph observations	. . .	jet-like ejections[f], narrow CMEs of width <90°[g]	CME	fast (>500 km s^{-1}) and wide (>90°) CMEs[l]
In situ observations in the solar wind	. . .	. . .	IP shock	IP shock occasionally followed by CME ejecta
Events/year	~1000	~1000	~10	~10

[a]Averaged over several events.
[b]Range measured in individual events.
[c]*Mason et al.* [2004].
[d]*Klecker et al.* [2006].
[e]*Leske et al.* [2005].
[f]*Wang et al.* [2006].
[g]*Kahler et al.* [2001].
[h]Energetic particle composition instruments in the 1970s–1980s did not have sufficient mass resolution to measure the $^3He/^4He$ ratio below the ~10% level, so it was simply assumed that the $^3He/^4He$ ratio in gradual SEPs would be similar to that measured in the presumed source material, i.e., the solar wind.
[i]*Desai et al.* [2006a].
[j]*Mazur et al.* [1999], *Möbius et al.* [1999], *Leske et al.* [2001].
[k]*Cane et al.* [2002].
[l]*Gopalswamy et al.* [2004].

chambers and neutron monitors [*Forbush*, 1946; *Meyer et al.*, 1956]. Such events, also known as ground level events or GLEs, were closely associated with the maximum of Hα flares on the Sun. Consequently, it was presumed that there was a causal relationship between the flare and the energetic particles observed at 1 AU. Later, however, on the basis of close association between SEP events and slow-drifting Type II and various Type IV radio bursts, *Wild et al.* [1963] proposed that the energetic particles might be accelerated at magnetohydrodynamic shock waves that typically accompanied the flares. In addition, *Lin* [1970] reported that the SEP events observed at 1 AU could essentially be grouped into two types: ''pure'' electron events closely associated with flares and metric Type III emission; and ''mixed'' events where protons, relativistic electrons, and flares were associated with Type II/IV radio events. On this basis *Lin* [1970] proposed two distinct acceleration processes for the pure and the mixed SEP events.

[5] Using Skylab observations, *Kahler et al.* [1978] noted a close association between CMEs and large solar proton events, suggesting that the CME could either create open field lines for flare particles to escape into the interplanetary medium or that the protons could be accelerated near a region above or around the outward moving ejecta far above the flare site. Subsequently, detailed analyses of flare durations, longitudinal distributions from multispacecraft observations, high-resolution ionic charge state and elemental composition measurements, and clearer associations with radio bursts led most researchers in the 1990s to accept the viewpoint that the SEP events observed at 1 AU belong to two classes: impulsive and gradual [e.g., *Kahler et al.*, 1978; *Cliver et al.*, 1982; *Kocharov*, 1983; *Kahler et al.*, 1984; *Luhn et al.*, 1984; *Mason et al.*, 1984; *Cane et al.*, 1986; *Reames*, 1988].

[6] In this two-class picture, as summarized in Table 1 [e.g., *Reames*, 1999; *Cliver*, 2000], gradual SEP events are longer-lasting (several days) and have larger fluences. These events are associated with Type II radio bursts and are characterized by coronal-like abundances and ionic charge states for Fe (Q~14). In contrast, the shorter duration (approximately a few hours) impulsive events have smaller fluences and are associated with impulsive x-ray flares and Type III radio bursts. These events are characterized by significant enhancements in ^{3}He, electrons, and heavy ions over the corresponding solar wind values and with Fe charge states up to ~20 [*Luhn et al.*, 1984]. Impulsive events are generally detected when the observer is magnetically connected to the flare site, while ions accelerated at the expanding large-scale CME-driven shocks populate magnetic field lines over a broad range of longitudes [*Cane et al.*, 1988]. This paradigm clearly distinguishes between two separate acceleration sites and mechanisms, both driven by explosive events on the Sun: diffusive acceleration of

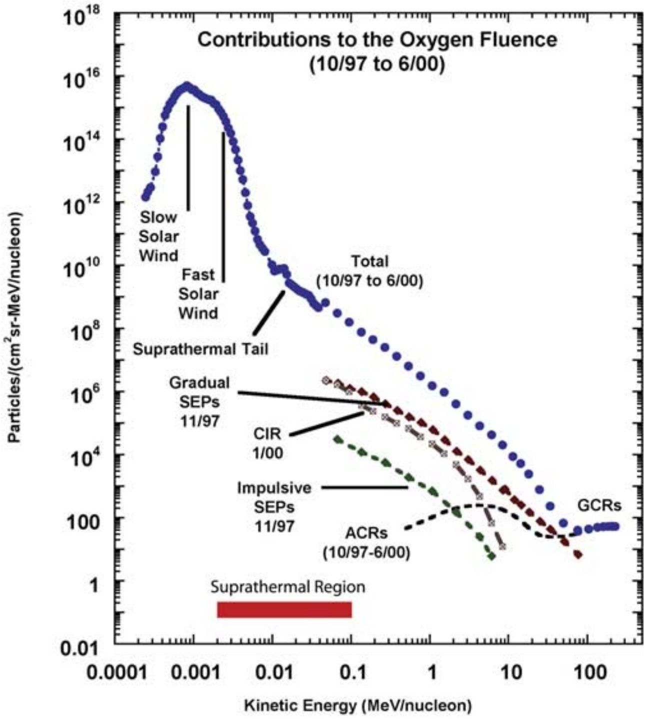

Figure 1. Contributions to oxygen fluences measured by several ACE instruments over a 3-year period. Also shown are representative energy spectra measured in various types of particle events [*Mewaldt et al.*, 2001]. The red bar denotes the suprathermal energy region between ~2 and 100 keV/nucleon.

ambient coronal or solar wind material at CME-driven coronal and IP shocks; and stochastic acceleration of coronal material heated up to ~10 MK during magnetic reconnection in solar flares.

[7] Since these earlier studies, instruments with greater sensitivity and resolution on board the Wind spacecraft [*Acuña et al.*, 1995] and the Advanced Composition Explorer (ACE) [*Stone et al.*, 1998a] during solar cycle 23 have provided major observational advances in terms of comparing the solar wind ion composition and its variations [*Gloeckler et al.*, 1992; *von Steiger et al.*, 2000] with the energy dependence and event-to-event variability of the ionic charge state, elemental, and isotopic composition in SEP events over a broad energy range [e.g., *Oetliker et al.*, 1997; *Mazur et al.*, 1999; *Möbius et al.*, 1999; *Cohen et al.*, 2005; *Desai et al.*, 2006a; *Klecker et al.*, 2006]. These new observations have made it possible to reexamine questions about the origin of the seed populations for shocks near 1 AU [*Desai et al.*, 2001, 2003; *Kucharek et al.*, 2003] and near the Sun [*Cohen et al.*, 1999; *Mason et al.*, 1999; *Desai et al.*, 2006a], reevaluate the relative roles of flares and CME-driven shocks [e.g., *Cohen et al.*, 1999; *Cane et al.*, 2003; *Tylka et al.*, 2005], and probe details of the effects of scattering near the coronal acceleration region and transport to 1 AU during individual events [*Cohen et al.*, 2005; *Tylka et al.*, 2005; *Mason et al.*, 2006].

[8] Table 1 summarizes our current understanding of SEP events. It is now clear that individual large SEP (LSEP) events often exhibit characteristics of both gradual and impulsive SEP events, and that the distinction between SEP events is blurred. The remainder of this section focuses on new observations from solar cycle 23 that have contributed significantly to our understanding of LSEP events.

2.2. LSEP Events of Solar Cycle 23

[9] In addition to the transient SEP events, observations at 1 AU show a continuous presence of intermediate-energy particles extending from suprathermal energies to >10 MeV/nucleon [*Mason et al.*, 1999, 2005; *Gloeckler*, 2003; *Desai et al.*, 2006b]. Figure 1 shows oxygen fluences from the solar wind to cosmic ray energies obtained by several ACE instruments from October 1997 – June 2000 [*Mewaldt et al.*, 2001]. The suprathermal energy region (red bar in Figure 1) is between ~2 and 100 keV/nucleon. Figure 1 also shows the energy spectra of various solar and interplanetary sources that can contribute to this energy region. In addition to these sources, the suprathermal pool also includes interstellar and inner source pickup ions and the heated solar wind [e.g., *Mason et al.*, 2005]. *Desai et al.* [2006b] reported that the suprathermal heavy ion composition near 1 AU is highly dynamic and varies with solar activity (CIR-like during solar minimum and SEP-like during solar maximum). The contributions from various sources to the suprathermal pool probably also varies on shorter (approximately hours) time scales. Presently, however, neither the mechanisms responsible for the acceleration of these particles are known [e.g., *Fisk and Gloeckler*, 2006] nor are the temporal and spatial properties of the various sources characterized.

[10] Since there is strong evidence that such suprathermal particles serve as the dominant source material for LSEP events [*Mason et al.*, 1999; *Desai et al.*, 2006a], it has become necessary to understand the origin and variability of these particles and how they affect the injection and acceleration processes at CME-driven shocks. Indeed, recent modeling work has shown that the puzzling increase in the Fe/O ratio with increasing energy above 10 MeV/nucleon can be understood in terms of preferential injection and shock drift acceleration (SDA) [e.g., *Forman and Webb*, 1985] of remnant flare suprathermals at quasi-perpendicular shocks. In this model, the diffusive acceleration of solar wind suprathermals at quasi-parallel shocks results in a systematic decrease in Fe/O ratio with increasing energy [*Tylka et al.*, 2005]. This contrasting behavior is shown in Figure 2 for the 24 August 2002 and 21 April 2002 events observed at ACE.

[11] While the *Tylka et al.* [2005] model clearly depends on shock geometry near the Sun and the presence of suprathermal flare seed populations to account for LSEP events, *Cane et al.* [2003, 2006] alternatively proposed that all LSEP events seen at 1 AU are a mixture of flare- and shock-accelerated populations and that (Figure 3) the relative contributions from these components depends on properties of the flare, the strength of the CME shock, and the observer's magnetic connection to the flare site. In this scenario, well-connected western hemisphere events associated with longer duration flares and weaker CME shocks are dominated by the flare-accelerated population above ~10 MeV/nucleon, causing the intensities to rise promptly and the Fe/O to increase significantly over the corresponding

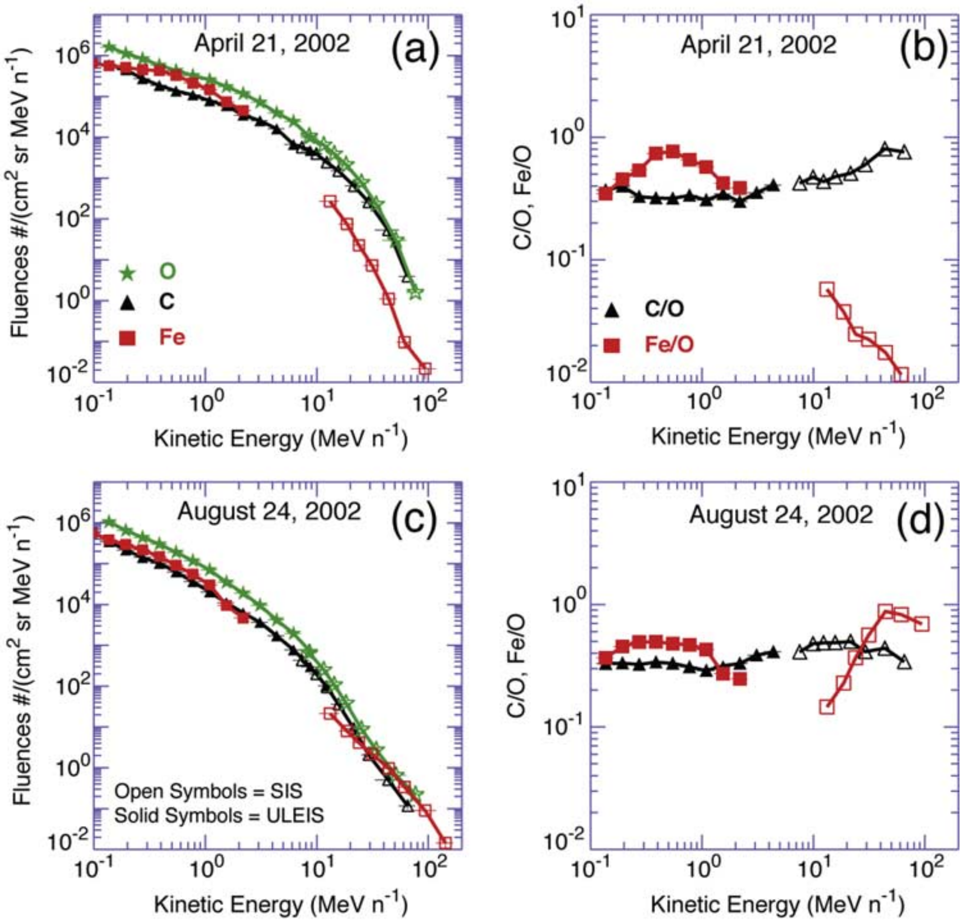

Figure 2. (a and c) O and Fe fluences versus kinetic energy. (b and d) Fe/O ratio versus kinetic energy for the 21 April 2002 and 24 August 2002 SEP events. Data are from ACE/ULEIS [*Mason et al.*, 1998] and ACE/SIS [*Stone et al.*, 1998b].

solar wind value (Figures 2 and 3a). On the other hand, poorly connected eastern hemisphere SEP events (Figure 3b) have broader time profiles and Fe/O ratios similar to or lower than the corresponding solar wind value. Finally, central meridian events (Figure 3c) have two components: a prompt rise early in the event due to flare particles, followed by a larger IP shock-accelerated component with Fe/O ~0.1 or less superposed on the flare population. On this basis, Cane et al. suggested that the CME shock was strong enough in the western hemisphere 21 April 2002 event to accelerate particles above ~10 MeV/nucleon and cause the Fe/O to decrease with increasing energy as shown in Figure 2.

[12] However, it is difficult to determine characteristics of the seed particle populations and CME shocks and to distinguish between the various acceleration processes

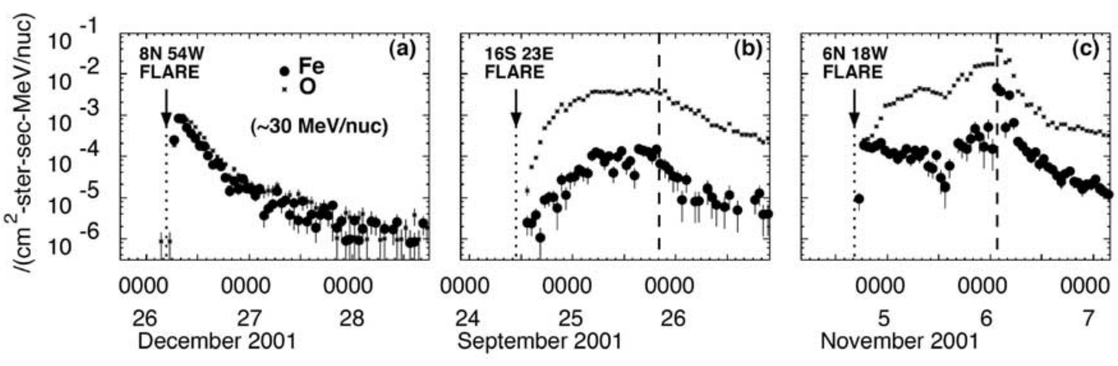

Figure 3. The ~30 MeV/nucleon Fe and O intensity profiles during three LSEP events of cycle 23 [*Cane et al.*, 2003]. These events are described as (a) prompt, (b) shock-accelerated, and (c) two-component.

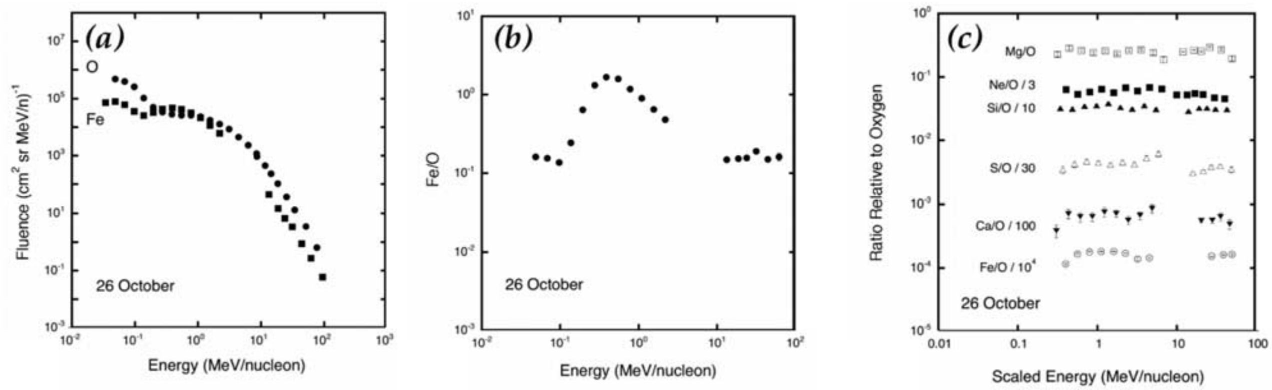

Figure 4. (a) Fe and O fluences, (b) Fe/O ratio versus kinetic energy in MeV/nucleon, and (c) heavy ion elemental abundances versus scaled kinetic energy for the 26 October 2003 SEP event [*Cohen et al.*, 2005] (see text for details).

occurring at the Sun on the basis of near-Earth data. This is primarily because the effects of scattering during acceleration, escape and propagation through the interplanetary medium smear out the temporal and spatial behavior [*Cohen et al.*, 2005; *Mason et al.*, 2006], potentially mixing particles from different acceleration sites. Indeed, *Cohen et al.* [2005] and *Mason et al.* [2006] suggested that the scattering of particles during acceleration or escape from the shock and/or during their propagation through the corona and the interplanetary medium play key roles in the compositional, spectral, and temporal variability of LSEP events. In particular, *Cohen et al.* [2005] noted that the breaks in the energy spectra for different species during each of the five LSEP events of October–November 2003 occur at the same value of the diffusion coefficient, κ, and used this to scale the energy spectra of various species. They suggested that the position of the spectral breaks and the resulting energy-dependent behavior is due to the rigidity dependence of the scattering mean free path in the vicinity of the shock acceleration region. *Zank et al.* [2000] showed that such rigidity dependence is consistent with a source of enhanced wave turbulence near the shock. An example of using the energy scaling to organize (flatten) the energy dependence of the heavy ion spectra is shown in Figure 4 for the 26 October 2003 event.

[13] In addition, *Mason et al.* [2006] pointed out that the dramatic variations in the Fe/O ratio at all energies between ~0.1 and 60 MeV/nucleon vanish in the majority (>70%) of the "prompt" western hemisphere SEP events that they surveyed by comparing the Fe intensities to the O intensities at approximately twice the Fe kinetic energy per nucleon. An example of such a comparison for the day 273, 1998 western hemisphere SEP event is shown in Figure 5. Note that the O intensity compared at twice the Fe energy results in nearly indistinguishable time histories. *Mason et al.* [2006] attributed the temporal behavior of the Fe/O ratio observed at the same kinetic energy per nucleon to the rigidity (or diffusion coefficient)-dependent scattering of

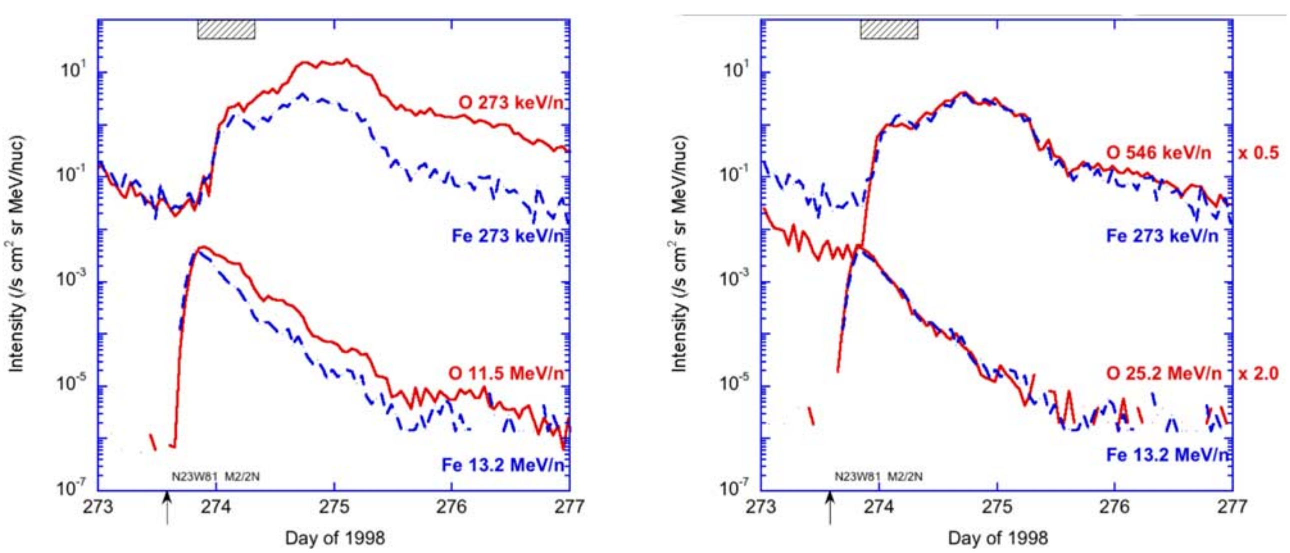

Figure 5. (left) Hourly averaged Fe (blue) and O (red) intensities at ~273 keV/nucleon and ~12 MeV/nucleon for the day 273, 1998 SEP event. (right) Fe intensities at the same energy, but the O intensities are at approximately twice the kinetic energy per nucleon. The O intensities are renormalized to facilitate comparison [*Mason et al.*, 2006].

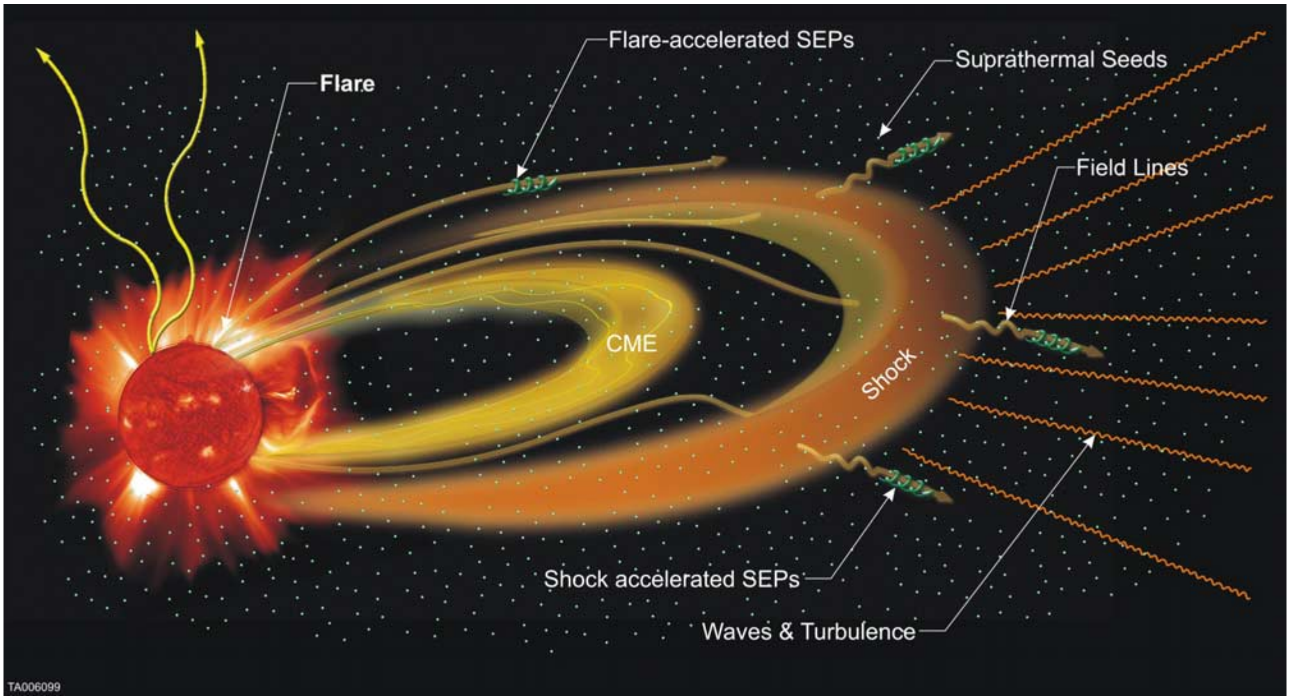

Figure 6. Cartoon summarizing our current understanding of the four distinct physical processes that are believed to contribute to large gradual SEP events (see text for details).

particles as they propagate through the corona and the interplanetary medium.

[14] In summary, LSEP observations of solar cycle 23 have raised the following important questions: (1) What physics determines the velocity or rigidity-dependent ordering of the heavy ion spectra, abundances, and time profiles in LSEP events? (2) Does such ordering depend on the location of the observer relative to the flare longitude and on CME shock geometry near the Sun? (3) How do flares contribute to LSEP events, i.e., do they provide seed particles or contribute directly? (4) What roles do particle scattering by waves and turbulence play during the acceleration/escape from the shock in the corona and during transport through the inner heliopshere? Table 1 and Figure 6 summarize these questions and show that the compositional, spectral and temporal variability during LSEP events of solar cycle 23 are believed to occur as a result of contributions from four different processes: (1) the reacceleration of remnant or fresh suprathermal ions from flares and prior gradual SEP events [*Mason et al.*, 1999; *Desai et al.*, 2006a; *Mewaldt et al.*, 2006], (2) the interplay between shock geometry and preferential injection of suprathermal solar wind or flare ions [*Tylka et al.*, 2005], (3) direct contributions from the accompanying flare [*Li and Zank*, 2005; *Cane et al.*, 2006], and (4) particle scattering in the corona and the interplanetary medium [*Cohen et al.*, 2005; *Mason et al.*, 2006]. Some of these ambiguities will undoubtedly be resolved in cycle 24 using observations from the twin-STEREO spacecraft, but the ultimate answers lie in making detailed in situ measurements as close to the Sun as possible where the effects of scattering and transport should be less prominent.

3. Energetic Ions Near the Earth's Bow Shock

3.1. Overview

[15] The Earth's bow shock has several unique features important in considering particle acceleration. Observations from Earth orbit have low relative speed between the spacecraft and shock, with high time resolution, which allows a detailed view of shock structure. Multispacecraft missions have enabled questions of temporal-spatial aliasing to be resolved so that accurate shock speed and orientation can be found. However, there are limitations when attempting

Table 2. Properties of Upstream Ion Events Near the Earth's Bow Shock

Property	Acceleration at Bow Shock	Magnetospheric Leakage
Composition	solar wind–like, high-charge-state C, Ne-S and Fe	low-charge-state ionospheric ions like O+, N+; high-charge-state solar wind ions
Energy spectra	exponential in E/q up to ∼150–200 keV/e	power laws extending up to ∼2 MeV
Electron association	up to ∼10s of keV at quasi-perpendicular portions of the bow shock	up to ∼ 1 MeV
Anisotropy	isotropic, diffuse, gyrating, beam-like, reflected	strong (up to 1000:1) sunward anisotropies

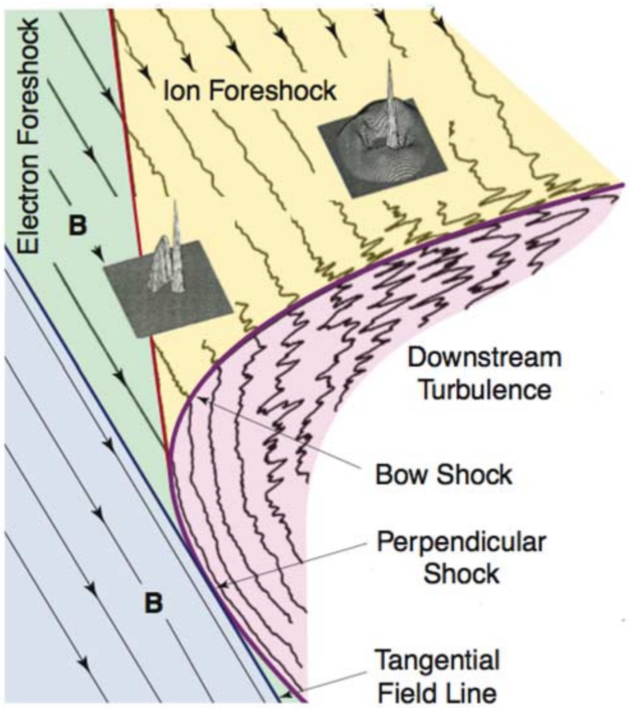

Figure 7. Schematic view of the bow shock and upstream foreshock as developed from observations taken close to the Earth. The solar wind flow direction is to the right, and the bow shock is represented by a curved line. The foreshock, largely upstream of the quasi-parallel shock, is downstream of the tangent field line and exhibits significant spatial structure. Just behind the tangent field line is the electron foreshock. Behind the ion foreshock boundary, field-aligned backstreaming ion distributions are typically observed. Deeper in the foreshock, close to the quasi-parallel shock, diffuse backstreaming ion distributions are observed. Two-dimensional velocity space relief plots are used to represent the field-aligned (close to the ion foreshock boundary) and the diffuse (close to the quasi-parallel shock) ion distributions. In these two-dimensional relief plots, the sharp peak corresponds to the solar wind [*Eastwood et al.*, 2005].

to carry out tests of particle acceleration theories. The shock surface has a relatively small radius of curvature (compared to IP shocks), which is important for the comparative study of quasi-perpendicular and quasi-parallel shock structure; however, when the motion of energetic particles is considered, the small size of the system means that different regions may interact, particularly in the foreshock. Observations do not sample the full extent of the foreshock upstream, and with the low speed of spacecraft relative to the bow shock, temporal changes depend primarily on reconfiguration of the shock/foreshock as solar wind conditions change. This creates difficulties in interpreting temporal or spatial changes in the data, e.g., the time scales associated with acceleration processes. Finally, the bow shock is relatively close to the obstacle off which it stands. Geomagnetic activity triggered by magnetopause reconnection increases the possibility of particles energized within the magnetosphere escaping and contributing to upstream distributions. An overview of the known properties of these distinct types of upstream ion events is provided in Table 2.

3.2. Global Morphology

[16] From the International Sun-Earth Explorer (ISEE) mission a view of the global morphology of the bow shock and foreshock was developed (Figure 7), which is still the framework for explaining observations (for a recent review, see *Eastwood et al.* [2005]). Table 3 summarizes the properties of the distinct types of ion populations observed upstream of the Earth's bow shock. The foreshock is structured by the convection of interplanetary magnetic field (IMF) lines, the velocity of energetic particles as they leave the shock, and the propagation of particles (whether scatter free or diffusive). The orientation of the foreshock is controlled by the solar wind magnetic field, with the upstream edge defined by the tangent field line. Particles with progressively lower energies traveling upstream from a point on the bow shock follow paths at greater angles to the magnetic field (if scattering is neglected). Moreover, the configuration of the bow shock changes from quasi-perpendicular to quasi-parallel as the field lines connect deeper into the foreshock, affecting the energies of particles leaving the shock.

[17] Behind the upstream foreshock edge, the foreshock contains electron beams with energies 1 - 10 keV that are seen close to, and just behind, the tangent field line where θ_{Bn} = 90. With deeper connection, lower-energy electrons are seen, including a heat flux from the downstream heated distribution [e.g., *Fitzenreiter*, 1995]. Low-energy field-aligned ion beams (FABs) are seen on field lines with deeper connection to the quasi-perpendicular bow shock. With still deeper connection where the magnetic field connects to the quasi-parallel bow shock, ions are seen with energies extending to 200 keV and distributions that are nearly isotropic. This latter class is the so-called diffuse ions. Although characterized as near isotropic at the shock, observations far upstream show a strong anisotropy for this energy range. Each foreshock region is associated with different wave types, but for energetic ions, the most important are the large-amplitude, ultralow-frequency (ULF) waves (period 5–20 s) seen in the quasi-parallel foreshock.

3.3. Field-Aligned Beams

[18] The region of Field-Aligned Beams (FABs) is distinct within the global morphology of the ion foreshock and is usually seen as a transition between unconnected solar wind and the more energetic diffuse ion region. The beams have low energy, seldom extending beyond 10 keV, with intrinsic (i.e., in the beam frame) perpendicular temperature anisotropy and densities typically 1% of the solar wind value. FABs are produced at the bow shock where θ_{Bn} is between 40° and 60°, but *Oka et al.* [2005] reported observations of a beam where the density decreased by more than an order of magnitude as θ_{Bn} increased to ~75°.

[19] There are other types of ion beams related to the FAB class. Intermediate ion beams have a slightly larger pitch angle spread and higher energies, while gyrating ion beams consist of an important gyrotropic component and are generally nongyrotropic [*Fuselier et al.*, 1986]. (The gyrating ion beam class should not be confused with the so-called

Table 3. Properties of Different Types of Upstream Ion Events Near Earth

Property	Foreshock Ions		Far Upstream Ions	
	Beam-Like	Diffuse	Magnetospheric Leakage	Bow Shock Accelerated
Duration	approximately a few minutes to 2 h	approximately a few minutes to 2 h	approximately a few minutes to 2 h	approximately a few minutes to 2 h
Temporal variations				
Intensity	abrupt onsets, associated with magnetic field direction changes and connection to quasi-perpendicular bow shock	e-folding distance of density gradient increases linearly with energy	abrupt onsets and decays	abrupt onsets and decays
Energy/velocity dependence	density decreases with peak energy	inverse velocity dispersion	all energies rise simultaneously and abruptly	all energies rise simultaneously and abruptly
Composition				
Elemental	He^{2+} deficient compared to solar wind	solar wind–like	ionospheric species, e.g., N^+, O^+	C-Fe similar to CIRs during solar minimum (C/O~0.75, Fe/O ~0.1) and similar to SEPs during solar maximum (C/O~0.4, Fe/O~0.2–0.5)
$^3He/^4He$	?	No	N/A	few isolated cases
Charge states	solar wind–like	solar wind–like	occasional presence of low-charge-state O and N; also include multiply charged solar wind ions	highly ionized O and C; solar wind–like for Fe
Energy dependence	none	?	none	?
Energy spectra				
Range	1–10 keV	Few keV up to ~150–200 keV/e	10s of keV up to ~1–2 MeV in total energy	10s of keV up to ~1–2 MeV in total energy
Shape	highly peaked spectra, some evidence of high-energy tail	exponentials in energy/charge	soft power laws with spectral indices ~4	soft power laws with spectral indices ~4
Anisotropy	beam-like in solar wind frame, perpendicular anisotropy in beam frame	diffuse, near isotropic close to bow shock	strong (up to ~1000:1) sunward streaming	strong (up to ~1000:1) sunward streaming
Electron Association	electron heat flux from bow shock	none	up to ~100 keV	~25% of events have electrons up to ~100 keV

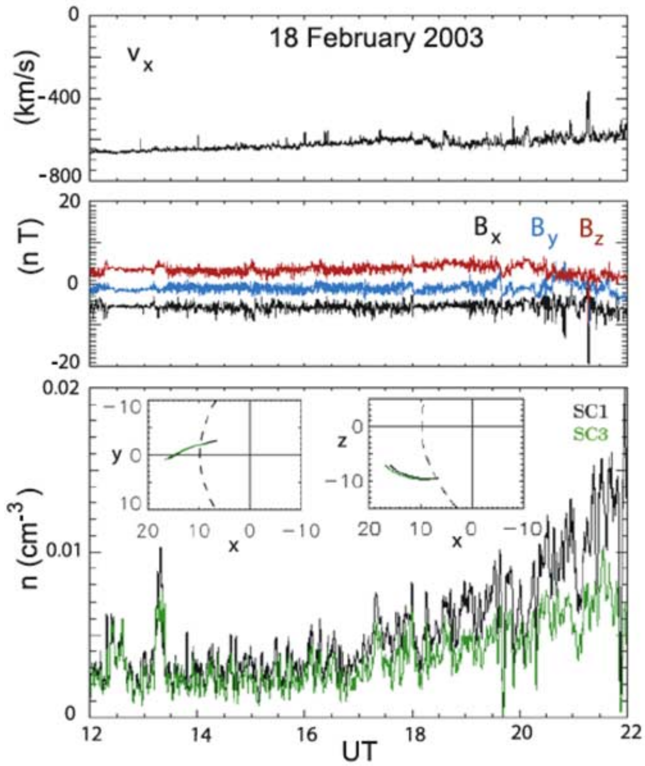

Figure 8. Cluster observations of spatial gradient in diffuse ions. (top) Solar wind velocity component Vx, (middle) magnetic field components Bx (black line), By (blue line), and Bz (red line) as measured on Cluster 1, and (bottom) partial ion density in the 24–32 keV energy range as measured at Cluster 1 (black line) and Cluster 3 (green line). Also shown in the bottom panel are projections of the spacecraft orbits and bow shock onto the x-y and x-z plane, respectively [*Kis et al.*, 2004].

reflected gyrating ions seen at the quasi-perpendicular shock.)

[20] Ion beams are a strong source of waves via linear instabilities. *Winske and Leroy* [1984], for example, present the linear theory and results of hybrid simulations of ion beam instabilities. These simulations indicate an evolution from beam-like to isotropic, which was suggested as a mechanism for the production of diffuse ions. Unlike diffuse ions, the FABs have low alpha particle relative abundance [*Ipavich et al.*, 1984, 1988], making them an unlikely source of diffuse ions. They may, however, have a role in seeding the quasi-parallel foreshock with ULF waves. The FAB region tends to have little ULF wave activity, but monochromatic ULF waves are associated with gyrating beams, with a distinct boundary between the two types of distributions [*Meziane et al.*, 2004].

3.4. Diffuse Ion Distributions

[21] Upstream diffuse ion distributions, with densities relative to the solar wind of 0.5–2% [*Trattner et al.*, 1994] and energies extending to about 200 keV/q, are associated with magnetic connection to the quasi-parallel portion of the bow shock. Velocity space distributions show a near isotropic shell extending from the energy of the solar wind [*Paschmann et al.*, 1981]. The energy spectra above 30 keV are well represented by exponentials in energy, and different species have similar spectra when plotted in terms of the ions' E/q. The abundance ratios of different species are constant when evaluated at the same E/q, with the alpha-to-proton ratio being close to the corresponding solar wind value [*Ipavich et al.*, 1984, 1988].

[22] In a statistical study, *Trattner et al.* [1994] found that the fluxes of the diffuse ions fall off exponentially with distance from the bow shock, with an e-folding distance varying from 3 R_E to 10 R_E between 10 keV and 67 keV for both protons and alpha particles. *Kis et al.* [2004], using Cluster data for a single event, were able to extract the spatial profile of energetic particle intensity and show that it followed an exponential fall-off, with e-folding distances varying between 0.5 and 2.8 R_E for the energy range 11 keV to 27 keV (Figure 8). The significant energy-dependent increase in the e-folding distance indicates that more energetic particles can escape more easily into the upstream region, leading to harder spectra and larger anisotropy further from the bow shock.

3.5. Magnetospheric Ions and Far Upstream Events

[23] Ion intensity enhancements of approximately a few keV up to ~1–2 MeV in energy have been routinely observed far upstream (>20 R_E) and outside of the ion foreshock regions since the 1960s [e.g., *Asbridge et al.*, 1968; *Sarris et al.*, 1976; *Scholer et al.*, 1979]. Such events are characterized by short durations (~1–2 h), steeply falling spectra ($j \propto E^{-4}$), large (>100:1) field-aligned sunward anisotropies [*Mitchell and Roelof*, 1983; *Müller-Mellin et al.*, 2007], and positive correlations with the solar wind speed and geomagnetic indices [e.g., *Desai et al.*, 2000]. Despite the wealth of information available, however, it is still not clear whether these ions are accelerated at the bow shock [e.g., *Lee*, 1982; *Trattner et al.*, 2003] or inside the Earth's magnetosphere [*Sheldon et al.*, 2003; *Anagnostopoulos et al.*, 2005; *Chen et al.*, 2005].

[24] In order to distinguish leaking magnetospheric ions from accelerated solar wind ions, measurements of ionic charge state are necessary, with low-charge-state ions usually magnetospheric in origin. It has been suggested that the majority of energetic (>50 keV) ions are of magnetospheric origin and that Fermi acceleration is not required to explain their energization [e.g., *Anagnostopoulos et al.*, 1986]. However, the less frequent presence of ionospheric species like N^+ and O^+ ions (simultaneous with diffuse ions) [e.g., *Möbius et al.*, 1986; *Christon et al.*, 2000; *Posner et al.*, 2002] indicates that Fermi acceleration near the bow shock must occasionally be accompanied by leakage from inside the magnetosphere. Strong evidence for upstream diffusion [*Kis et al.*, 2004] also makes it is difficult to argue categorically that Fermi acceleration does not operate at the bow shock.

[25] Simultaneous IMP measurements of ion events inside the magnetosphere and in the upstream region led *Sarris et al.* [1978, 1987] to propose that the events observed upstream of Earth probably originated from inside the magnetosphere. In contrast, *Scholer et al.* [1981], using ISEE-1 and –3 data, reported that the upstream ion distributions look substantially different close to the bow shock and far upstream. They pointed out that some of the diffuse

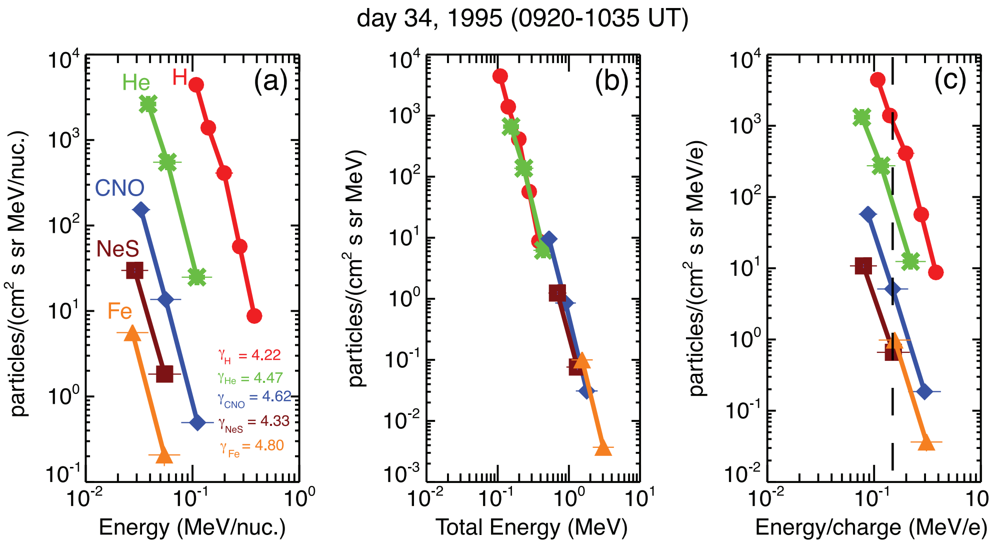

Figure 9. Differential energy spectra for all species during an upstream event measured plotted versus (a) energy/nucleon, (b) total energy, and (c) energy/charge (assuming solar wind charge states). The quantity γ is the power law spectral index, and the associated subscript denotes the species. Uncertainties in the values of γ are $\leq$30%. Notice the ordering of the energy spectra of different species as a single power law in total energy in Figure 9b, indicating that the higher-energy portion (>500 keV) of the total energy spectrum is essentially dominated by solar wind–like ion species like NeS and Fe. The dashed vertical line in Figure 9c is drawn at 150 keV/q to identify the predicted upper limit of the Fermi acceleration process of *Lee* [1982] (taken from *Desai et al.* [2000]).

ions could leak into the upstream region and then travel mostly scatter-free owing to the lower wave activity, leading to more anisotropic distributions [*Mitchell and Roelof*, 1983]. On the basis of this, Scholer et al. suggested that the locally accelerated diffuse population could be the source of the highly anisotropic distributions seen far upstream.

[26] Observations far upstream of the bow shock from such spacecraft as Wind, ACE and STEREO provide a different perspective on shock-associated energetic particles. Of particular relevance are the results of *Mason et al.* [1996] and *Desai et al.* [2000], which showed that the high-energy portion (above ~500 keV in total energy) of the energy spectra in upstream events was dominated by heavier solar wind–like ions such as CNO, NeS and Fe (Figure 9). *Desai et al.* [2006c] showed that the heavy ion composition in far upstream events above ~100 keV depends on the phase of the solar cycle and is essentially dominated by solar wind, CIR or SEP-like material. These new composition results appear to favor the acceleration of suprathermal ions of solar or interplanetary origin at the bow shock as the dominant mechanism.

[27] Finally, in studying the simultaneous occurrence of far upstream events, many independent studies have concluded that upstream ions probably originate from a large source region perhaps covering the entire size of the bow shock [e.g., *Scholer et al.*, 1981; *Haggerty et al.*, 1999, 2000; *Dwyer et al.*, 2000; *Desai et al.*, 2008] and propagate in large spatial structures in the upstream region [e.g., *Sanderson et al.*, 1981; *Haggerty et al.*, 1999, 2000; *Dwyer et al.*, 2000; *Desai et al.*, 2008]. Simultaneous observations of upstream events from STEREO-A, ACE and Wind [*Desai et al.*, 2008] have identified these spatial structures (~0.03 AU) to be large-amplitude, anti-sunward propagating Alfvén waves embedded within high-speed solar wind flows associated with corotating interaction regions.

[28] In summary, two prominent questions remain unanswered: (1) What is the relative contribution of magnetospheric leakage to far upstream ion events? *Desai et al.* [2000] report that 25% of events are accompanied by 35 keV electrons (a tracer of magnetospheric leakage). On the other hand, the majority of upstream events probably originate on the dawnside of the bow shock, which is difficult to reconcile with the assertion that leakage from the magnetosphere will occur preferentially on the duskside. (2) When do these events occur? *Desai et al.* [2000, 2006c] also found a correlation between their frequency with solar cycle (more frequent during solar minimum), possibly indicating a link to geomagnetic activity. *Posner et al.* [2002] found some correlation with geomagnetic activity for events far upstream, but *Trattner et al.*'s [1994] statistical survey found no correlation with southward Bz. Other open questions relate to whether leaked particles are passive in waves and field structures governed by shock-accelerated particles, and the relative importance of large amplitude Alfvén waves. The main challenge for any model of far upstream ion production is to quantitatively account for the variety of complex observations in these events [*Desai et al.*, 2000, 2006c, 2008].

4. Particle Acceleration Mechanisms

4.1. Fast Fermi or SDA

[29] A particle from the solar wind distribution reflected from the shock back upstream will gain energy in the normal incidence frame via the motional electric field. Reflection by magnetic mirroring successfully estimates

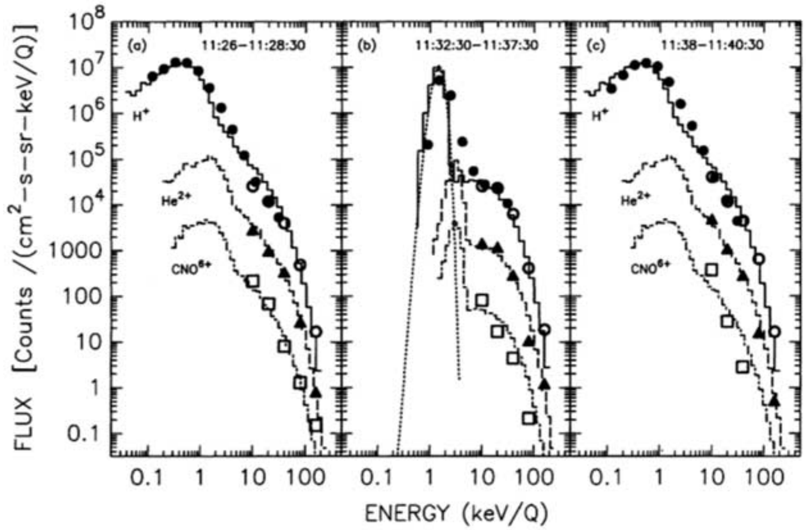

Figure 10. Monte Carlo simulation fits to spectra measured downstream and upstream of the Earth's bow shock by the AMPTE/IRM spacecraft. Filled and open circles are protons, triangles are He^{2+}, and squares are CNO^{6+}. All parameters are the same in Figures 10a–10c except for the observation position and the normalization. The normalization is determined from the observations and Figures 10a and 10c show downstream spectra, while Figure 10b shows upstream spectra. Figure 10 is from *Ellison et al.* [1990] (reproduced by permission of the AAS), which should be referred to for a complete description of the model and parameters.

ion beam speeds [*Sonnerup*, 1969] but not density. The assumption of adiabatic invariance is also difficult to justify for suprathermal particles. In SDA the energy gain is from drift along the shock surface in the direction of the motional electric field. Simulations have shown that this mechanism is viable for producing beams consistent with the observed energies and reflected fractions [*Burgess*, 1987]. Test particle simulation of an observed event showed that the multiple encounter trajectory behavior of a SDA mechanism was a satisfactory explanation [*Oka et al.*, 2005]. This latter study also found a density variation with θ_{Bn} consistent with the simulation results.

[30] *Tanaka et al.* [1983] proposed a model for FAB generation by leakage from the heated magnetosheath distribution. This is not supported by the observations and simulations, which show that isotropization occurs close to the shock surface and not some distance behind it. Observations taken within the shock layer [*Möbius et al.*, 2001] show a field-aligned beam developing directly out of the reflected-gyrating distribution. *Kucharek et al.* [2004] report a simultaneous dual spacecraft observation across the shock when a FAB is seen upstream. The downstream distribution has an insufficient level of phase space density to explain the observed upstream beam.

4.2. First-Order Fermi or Diffusive Acceleration

[31] The isotropy of the distributions at, and downstream of, the shock suggests that Fermi acceleration (also called first-order Fermi or diffusive shock acceleration) is responsible in some measure for the particle energization. This process has been broadly studied in the context of cosmic ray acceleration and shocks in interplanetary space [*Forman and Webb*, 1985; *Scholer*, 1985; *Jones and Ellison*, 1991].

[32] The theory of Fermi acceleration is usually treated as a diffusion-convection problem for the energetic particle distribution function, coupling the energetic particles with wave-particle scattering to the compression across the shock [e.g., *Forman and Webb*, 1985]. If the plasma flow and shock compression are fixed, then planar, steady state theories predict power law spectra with a slope that depends only on the shock compression independent of the species. In quasi-linear models [*Lee*, 1982, 1983], the spectrum of scattering waves is developed self-consistently with the spectrum of energetic particles, which are themselves assumed to be generating the waves resonantly [*Ng et al.*, 2003].

[33] Any application of Fermi acceleration to explain the energetic particle distributions at the Earth's bow shock and CME-driven IP shocks must account for the exponential spectra and their organization by E/q [*Trattner et al.*, 1994] or ion rigidity [*Cohen et al.*, 2005]. Some form of loss mechanism is required, and two possibilities have been suggested. *Lee*'s [1982] quasi-linear theory uses a finite-sized shock with particle loss at the sides of the acceleration region by perpendicular diffusion. With this assumption, and the use of diffusion coefficients derived from quasi-linear theory, the required E/q organization of the spectra can be recovered. The calculated wave energy power is also broadly consistent with the observations [*Trattner et al.*, 1994].

[34] An alternative loss process is the so-called free escape boundary (FEB) somewhere upstream of the shock. This has been employed in Monte Carlo simulations of diffusive acceleration at the Earth's bow shock and at CME-driven IP shocks [e.g., *Ellison et al.*, 1990; *Li et al.*, 2003, 2005]. The use of a FEB has some justification based on the observation far upstream of highly anisotropic distributions [e.g., *Desai et al.*, 2000]. Comparison with data from AMPTE/IRM upstream and downstream of the bow shock

Table 4. Observational Properties of Large Gradual SEP Events and Upstream Events

Property	Large Solar Energetic Particle Events (SEPs)	Upstream Events: Foreshock	Upstream Events: Far Upstream
Duration	several hours to a few days	approximately a few minutes to 2 h	approximately a few minutes to 2 h
Temporal variations			
Intensity	Depends on magnetic connection between observer and solar source region. Well-connected western hemisphere events: prompt rise followed by slow decay; central meridian events: Prompt rise followed by a local increase around shock passage; eastern events: gradual increase with a peak prior to shock arrival.	e-folding distance of density gradient increases linearly with energy	abrupt onsets and decays
Energy/velocity dependence	normal velocity dispersion for well-connected events	inverse velocity dispersion	all energies rise simultaneously and abruptly
Fe/O ratio	increases initially and then decreases near shock passage	?	?
Composition			
Elemental	C-Fe systematically enhanced relative to the corona according to M/Q ratio, but exhibit no systematic relationship as a function of M/Q ratio when compared with the solar wind	solar wind–like	C-Fe similar to CIRs during solar minimum (C/O$\sim$0.75, Fe/O $\sim$0.1) and similar to SEPs during solar maximum (C/O$\sim$0.4, Fe/O $\sim$0.2–0.5)
$^3He/^4He$ ratio	enhanced between $\sim$4 and 150 times that measured in the ambient corona or the solar wind	no	few isolated cases
Charge states	energy-dependent increase in Fe Q-state; above 10 MeV/nucleon, Q reaches $\sim$20 in some events	solar wind–like	solar wind–like for Fe; occasional presence of low-charge-state O and N
Energy dependence	Fe/O increases, decreases, or remains constant with increasing energy	?	none
Energy spectra			
Range	few keV up to GeV	few keV up to $\sim$150–200 keV/e	10s of keV up to $\sim$1–2 MeV in total energy
Shape	power laws modulated by exponentials or double power laws; spectral breaks determined by the rigidity dependence of the diffusion coefficient	exponentials in energy/charge	soft power laws with spectral indices $\sim$4
Anisotropy	field-aligned away from the Sun at the start of the event; reverses direction when IP shock passes over the spacecraft	diffuse, isotropic, gyrating, reflected, beam-like	strong (up to $\sim$1000:1) sunward streaming
Electron Association	$\sim$10 s of keV up to approximately a few MeV	no	up to $\sim$100 keV

shows good agreement between observations and the results of Monte Carlo modeling (Figure 10).

[35] In greater than one dimension another effect may have to be considered. For a finite shock, and an inclined field, each field line has only a finite time of connection to the shock which corresponds to a finite maximum in particle energy. It is possible that the FEB in one dimension has the same effect as the time of connection for a shock of finite extent [*Scholer et al.*, 1999].

[36] A major question arises from the so-called injection problem: How do some particles that start in the thermal distribution participate in the diffusive shock acceleration process and gain enough energy to be considered energetic? The injection of thermal solar wind ions has plagued our theoretical understanding of shock acceleration for several decades because of two reasons: (1) solar wind ions are highly anisotropic and the diffusive approximation becomes invalid, and (2) solar wind ions are convected away from the shock by the upstream solar wind flow, depriving them of sufficient speeds to return to the shock and participate in the acceleration process.

[37] Standard theories solve the diffusion-convection equation by simply assuming a given injection rate at a given energy at the shock, i.e., they inject a mono-energetic seed population. In contrast, Monte Carlo simulations do not have an ad hoc injection and assume that the scattering

Table 5. Comparison Between CME-Related Large SEP Events and Upstream Ion Events Near the Earth's Bow Shock

Property	Large Solar Energetic Particles (LSEPs)	Upstream Events
Acceleration site	CME-driven coronal and interplanetary shocks	Earth's bow shock
Source material	ambient coronal or solar wind plasma, suprathermals from the heated solar wind and previous flares and CME-shock-related SEP events	ambient solar wind, suprathermals from the heated solar wind, previous flares and CME-shock-related SEP events, and CIR events
Injection and acceleration	diffusive shock acceleration	diffusive shock acceleration
Transport	diffusive	diffusive in the foreshock regions, scatter-free in the far upstream regions

law is valid down to thermal energies, thereby making the injection process diffusive, just like the acceleration process. Hybrid plasma simulations (kinetic ions, fluid electrons) demonstrate that the diffuse ions start their energization with a reflection-like interaction with the shock [*Kucharek and Scholer*, 1991]. This implies that the first step to injection occurs within the shock layer itself, so that the suprathermal particles are an integral part of the quasi-parallel shock and strongly relate to other features of the shock such as large amplitude magnetic pulsations and intermittent specular reflection [*Burgess et al.*, 2005].

[38] *Giacalone et al.* [1993] showed how injection proceeds by particle interaction with the large amplitude magnetic pulsations within the quasi-parallel shock. Energy spectra in agreement with diffusive acceleration theory, at least over a restricted energy range, were found. Later, very large simulations of the parallel shock [*Giacalone*, 2004] studied the effect of a FEB at a fixed distance from the shock. Energetic particle fluxes decayed to a constant value upstream, suggesting an increase of the mean free path with distance upstream of the shock and a reduction in the maximum energy. This is similar to the transition to approximately scatter-free propagation for energetic particles seen far upstream of the bow shock.

[39] Recent observations provide compelling evidence for the injection of suprathermal seed populations near the Earth's bow shock [*Desai et al.*, 2006c] and at CME-driven IP shocks [*Desai et al.*, 2001; *Kucharek et al.*, 2003], advancing the possibility that the "injection problem" for diffusive shock acceleration may not be as theoretically challenging as previously believed. Indeed, the suprathermal ions are likely to be injected into shock acceleration processes more efficiently when compared with the more abundant solar wind ions [*Kucharek and Scholer*, 1995].

[40] To date, predictions of the diffusive shock acceleration theory have been confirmed for a handful of CME-driven IP shocks [e.g., *Decker*, 1981; *Kennel et al.*, 1986; *Sanderson et al.*, 1985; *Lario et al.*, 2005b; *Zank et al.*, 2006]. In contrast, the energetic particle observations near the majority of IP shocks appear to be at odds with theoretical predictions [e.g., *Desai et al.*, 2004]. CME shocks also evolve dynamically and typically decrease in strength as they propagate through the solar corona and the interplanetary medium, which limits the ability of many of the shocks that produce SEPs near the Sun to accelerate particles by the time they reach 1 AU [*Lario et al.*, 2005a]. To fully understand the observed SEP properties at 1 AU and beyond will require time-dependent, multidimensional global simulations of CME shocks and SEP acceleration that inject realistic seed populations and employ self-consistent wave-particle interactions, including shock heating and dissipation mechanisms.

5. Summary and Concluding Remarks

[41] Table 4 compares and contrasts in detail the properties of large CME-related gradual SEP events with those of the upstream ions. Of particular interest are the temporal behavior, compositional and spectral properties, particle anisotropies, and association with energetic electrons. Recent measurements from missions such as ACE, Wind, SoHO, Cluster, Polar, Geotail and SAMPEX have filled in numerous gaps in our understanding of the generation of these particle populations. However, we are still unable to develop quantitative predictive models of radiation hazardous SEPs and upstream ion events. Table 5 summarizes our current understanding of the four main questions relating to these populations.

[42] On the basis of detailed case studies and general statistical surveys of observations of upstream ion events, large gradual SEPs and IP shock-associated ESP events obtained over the last five decades, we conclude that diffusive shock acceleration is the most plausible mechanism for particle energization at CME-driven coronal and IP shocks as well as at the Earth's bow shock. However, despite recent, major theoretical advances, many important questions regarding SEPs and upstream ions near Earth remain unanswered. This is because both the SEP and upstream ion measurements are smeared by a confluence of poorly understood physical effects whose contributions can vary with time and location. These effects include (1) the physical properties of the shocks [*Burgess et al.*, 2005; *Bale et al.*, 2005; *Manchester et al.*, 2005; *Tylka et al.*, 2005]; (2) the nature of wave-particle interactions and the type of turbulence present near the shocks [*Ng et al.*, 2003; *Bamert et al.*, 2004; *Li et al.*, 2005]; (3) the kinetic processes by which the shocks heat the plasma and dissipate their energy [*Wilson et al.*, 2007; *Korreck et al.*, 2007]; (4) the distribution and composition of the seed populations available for acceleration [*Desai et al.*, 2006b; *Fisk and Gloeckler*, 2006, 2007; *Mewaldt et al.*, 2006]; (5) the type of injection and acceleration processes involved [*Ellison et*

al., 1990; *Tylka and Lee*, 2006; *Giacalone and Kóta*, 2006]; and (6) the manner in which the interplanetary medium affects particle transport to the observation point [*Cohen et al.*, 2005; *Mason et al.*, 2006]. Only by understanding the behavior of each of these processes and untangling their relative contributions to large gradual SEPs and upstream ion events will it be possible to construct accurate predictive models of particle injection and acceleration at CME shocks and the Earth's bow shock.

[43] **Acknowledgments.** Work at SwRI is partially supported by NSF grants ATM-0550960 and ATM-0551127 and NASA grants: NNG05GM88G, NNG05GQ94G, NNX07AC12G, NNX07AG85G, NNX07AP69G, and NNX08AK87G. D.B. acknowledges useful discussions with M. Scholer.

[44] Amitava Bhattacharjee thanks the reviewers for their assistance in evaluating this paper.

References

Acuña, M. H., K. W. Ogilvie, D. N. Baker, S. A. Curtis, D. H. Fairfield, and W. H. Mish (1995), The Global Geospace Science Program and its investigations, *Space Sci. Rev.*, *71*(1–4), 5–21, doi:10.1007/BF00751323.

Anagnostopoulos, G. C., E. T. Sarris, and S. M. Krimigis (1986), Magnetospheric origin of energetic (at least 50 keV) ions upstream of the bow shock: The October 31, 1977, event, *J. Geophys. Res.*, *91*, 3020–3028, doi:10.1029/JA091iA03p03020.

Anagnostopoulos, G. C., E. Efthymiadis, E. T. Sarris, and S. M. Krimigis (2005), Evidence and features of magnetospheric particle leakage on days 30–35, 1995: Wind, Geotail, and IMP 8 observations compared, *J. Geophys. Res.*, *110*, A10203, doi:10.1029/2004JA010827.

Asbridge, J. R., S. J. Bame, and I. B. Strong (1968), Outward flow of protons from the Earth's bow shock, *J. Geophys. Res.*, *73*, 5777, doi:10.1029/JA073i017p05777.

Bale, S. D., et al. (2005), Quasi-perpendicular shock structure and processes, *Space Sci. Rev.*, *118*(1–4), 161–203, doi:10.1007/s11214-005-3827-0.

Bamert, K., R. Kallenbach, N. F. Ness, C. W. Smith, T. Terasawa, M. Hilchenbach, R. F. Wimmer-Schweingruber, and B. Klecker (2004), Hydromagnetic wave excitation upstream of an interplanetary traveling shock, *Astrophys. J.*, *601*(1), L99–L102, doi:10.1086/381962.

Burgess, D. (1987), Simulations of backstreaming ion beams formed at oblique shocks by direct reflection, *Ann. Geophys.*, *5*, 133–145.

Burgess, D., et al. (2005), Quasi-parallel shock structure and processes, *Space Sci. Rev.*, *118*, 205–222, doi:10.1007/s11214-005-3832-3.

Cane, H. V., R. E. McGuire, and T. T. von Rosenvinge (1986), Two classes of solar energetic particle events associated with impulsive and long-duration soft X-ray flares, *Astrophys. J.*, *301*, 448, doi:10.1086/163913.

Cane, H. V., D. V. Reames, and T. T. von Rosenvinge (1988), The role of interplanetary shocks in the longitude distribution of solar energetic particles, *J. Geophys. Res.*, *93*, 9555–9567, doi:10.1029/JA093iA09p09555.

Cane, H. V., W. C. Erickson, and N. P. Prestage (2002), Solar flares, type III radio bursts, coronal mass ejections, and energetic particles, *J. Geophys. Res.*, *107*(A10), 1315, doi:10.1029/2001JA000320.

Cane, H. V., T. T. von Rosenvinge, C. M. S. Cohen, and R. A. Mewaldt (2003), Two components in major solar particle events, *Geophys. Res. Lett.*, *30*(12), 8017, doi:10.1029/2002GL016580.

Cane, H. V., R. A. Mewaldt, C. M. S. Cohen, and T. T. Rosenvinge (2006), Role of flares and shocks in determining solar energetic particle abundances, *J. Geophys. Res.*, *111*, A06S90, doi:10.1029/2005JA011071.

Chen, J., T. A. Fritz, and R. B. Sheldon (2005), Multiple spacecraft observations of energetic ions during a high solar wind pressure event, *J. Geophys. Res.*, *110*, A11212, doi:10.1029/2005JA011043.

Christon, S. P., M. I. Desai, T. E. Eastman, G. Gloeckler, S. Kokubun, A. T. Y. Lui, R. W. McEntire, E. C. Roelof, and D. J. Williams (2000), Low-charge-state heavy ions upstream of Earth's bow shock and sunward flux of ionospheric O^{+1}, N^{+1}, and O^{+2} ions: Geotail observations, *Geophys. Res. Lett.*, *27*, 2433–2436, doi:10.1029/2000GL000039.

Cliver, E. W. (2000), Acceleration and transport of energetic particles observed in the heliosphere, edited by R. A. Mewaldt et al., *AIP Conf. Proc.*, 528, 21.

Cliver, E. W., S. W. Kahler, M. A. Shea, and D. F. Smart (1982), Injection onsets of 2 GeV protons, 1 MeV electrons, and 100 keV electrons in solar cosmic ray flares, *Astrophys. J.*, *260*, 362, doi:10.1086/160261.

Cohen, C. M. S., A. C. Cummings, R. A. Leske, R. A. Mewaldt, E. C. Stone, B. L. Dougherty, M. E. Wiedenbeck, E. R. Christian, and T. T. von Rosenvinge (1999), Inferred charge states of high energy solar particles from the Solar Isotope Spectrometer on ACE, *Geophys. Res. Lett.*, *26*, 149, doi:10.1029/1998GL900218.

Cohen, C. M. S., E. C. Stone, R. A. Mewaldt, R. A. Leske, A. C. Cummings, G. M. Mason, M. I. Desai, T. T. von Rosenvinge, and M. E. Wiedenbeck (2005), Heavy ion abundances and spectra from the large solar energetic particle events of October–November 2003, *J. Geophys. Res.*, *110*, A09S16, doi:10.1029/2005JA011004.

Decker, R. B. (1981), The modulation of low-energy proton distributions by propagating interplanetary shock waves: A numerical simulation, *J. Geophys. Res.*, *86*, 4537–4554, doi:10.1029/JA086iA06p04537.

Desai, M. I., G. M. Mason, J. R. Dwyer, J. E. Mazur, T. T. von Rosenvinge, and R. P. Lepping (2000), Characteristics of energetic (>30 keV/nucleon) ions observed by the Wind/STEP instrument upstream of the Earth's bow shock, *J. Geophys. Res.*, *105*, 6178, doi:10.1029/1999JA900406.

Desai, M. I., G. M. Mason, J. R. Dwyer, J. E. Mazur, C. W. Smith, and R. M. Skoug (2001), Acceleration of ^{3}He nuclei at interplanetary shocks, *Astrophys. J.*, *553*, L89, doi:10.1086/320503.

Desai, M. I., G. M. Mason, J. R. Dwyer, J. E. Mazur, R. E. Gold, S. M. Krimigis, R. M. Skoug, and C. W. Smith (2003), Evidence for a suprathermal seed population of heavy ions accelerated by interplanetary shocks near 1 AU, *Astrophys. J.*, *588*, 1149, doi:10.1086/374310.

Desai, M. I., et al. (2004), Spectral properties of heavy ions associated with the passage of interplanetary shocks at 1 AU, *Astrophys. J.*, *611*(2), 1156–1174, doi:10.1086/422211.

Desai, M. I., G. M. Mason, R. E. Gold, S. M. Krimigis, C. M. S. Cohen, R. A. Mewaldt, J. E. Mazur, and J. R. Dwyer (2006a), Heavy ion abundances in large solar energetic particle events and their implications for the seed population, *Astrophys. J.*, *649*, 470–489, doi:10.1086/505649.

Desai, M. I., G. M. Mason, J. E. Mazur, and J. R. Dwyer (2006b), Solar cycle variations in the composition of the suprathermal heavy ion population near 1 AU, *Astrophys. J.*, *645*, L81–L84, doi:10.1086/505935.

Desai, M. I., G. M. Mason, J. E. Mazur, and J. R. Dwyer (2006c), Origin of heavy ions in upstream events near the Earth's bow shock, *Geophys. Res. Lett.*, *33*, L18104, doi:10.1029/2006GL027277.

Desai, M. I., G. M. Mason, R. Müller-Mellin, A. Korth, U. Mall, J. R. Dwyer, and T. T. von Rosenvinge (2008), The spatial distribution of upstream ion events from the Earth's bow shock measured by ACE, Wind, and STEREO, *J. Geophys. Res.*, *113*, A08103, doi:10.1029/2007JA012909.

Dwyer, J. R., G. M. Mason, M. I. Desai, J. E. Mazur, and T. T. von Rosenvinge (2000), The spatial distribution of ion events measured far upstream of the Earth's bow shock by ACE/ULEIS and Wind/STEP, *Geophys. Res. Lett.*, *27*, 65, doi:10.1029/1999GL003670.

Eastwood, J. P., E. A. Lucek, C. Mazelle, K. Meziane, Y. Narita, J. Pickett, and R. A. Treumann (2005), The foreshock, *Space Sci. Rev.*, *118*, 41–94, doi:10.1007/s11214-005-3824-3.

Ellison, D. C., E. Möbius, and G. Paschmann (1990), Particle injection and acceleration at Earth's bow shock-Comparison of upstream and downstream events, *Astrophys. J.*, *352*(1), 376–394, doi:10.1086/168544.

Fisk, L. A., and G. Gloeckler (2006), The common spectrum for accelerated ions in the quiet-time solar wind, *Astrophys. J.*, *640*(1), L79–L82, doi:10.1086/503293.

Fisk, L. A., and G. Gloeckler (2007), Acceleration and composition of solar wind suprathermal tails, *Space Sci. Rev.*, *130*(1–4), 153–160, doi:10.1007/s11214-007-9180-8.

Fitzenreiter, R. J. (1995), The electron foreshock, *Adv. Space Res.*, *15*(8–9), 9–27, doi:10.1016/0273-1177(94)00081-B.

Forbush, S. E. (1946), Three unusual cosmic-ray increases possibly due to charged particles form the Sun, *Phys. Rev.*, *70*, 771, doi:10.1103/PhysRev.70.771.

Forman, M. A., and G. M. Webb (1985), Acceleration of energetic particles, in *Collisionless Shocks in the Heliosphere: A Tutorial Review*, *Geophys. Monogr. Ser.*, vol. 34, edited by R. G. Stone and B. T. Tsurutani, pp. 91–114, AGU, Washington, D.C.

Fuselier, S. A., M. F. Thomsen, J. T. Gosling, S. J. Bame, and C. T. Russell (1986), Gyrating and intermediate ion distributions upstream from the Earth's bow shock, *J. Geophys. Res.*, *91*, 91–99, doi:10.1029/JA091iA01p00091.

Giacalone, J. (2004), Large-scale hybrid simulations of particle acceleration at a parallel shock, *Astrophys. J.*, *609*, 452–458, doi:10.1086/421043.

Giacalone, J., and J. Kóta (2006), Acceleration of solar-energetic particles by shocks, *Space Sci. Rev.*, *124*(1–4), 277–288, doi:10.1007/s11214-006-9110-1.

Giacalone, J., D. Burgess, S. J. Schwartz, and D. C. Ellison (1993), Ion injection and acceleration at parallel shocks-Comparisons of self-consistent plasma simulations with existing theories, *Astrophys. J.*, *402*, 550–559, doi:10.1086/172157.

Gloeckler, G. (2003), Ubiquitous suprathermal tails on the solar wind and pickup ion distributions, in *Solar Wind Ten: Proceedings of the Tenth*

International Solar Wind Conference, *AIP Conf. Proc.*, 679, 583, doi:10.1063/1.1618663.
Gloeckler, G., J. Geiss, H. Balsiger, P. Bedini, J. C. Cain, J. Fisher, L. A. Fisk, A. B. Galvin, F. Gliem, and D. C. Hamilton (1992), The solar wind ion composition spectrometer, *Astron. Astrophys. Suppl. Ser.*, *92*, 267.
Gopalswamy, N., S. Yashiro, S. Krucker, G. Stenborg, and R. A. Howard (2004), Intensity variation of large solar energetic particle events associated with coronal mass ejections, *J. Geophys. Res.*, *109*, A12105, doi:10.1029/2004JA010602.
Haggerty, D. K., M. I. Desai, G. M. Mason, J. R. Dwyer, R. E. Gold, S. M. Krimigis, J. E. Mazur, and T. T. von Rosenvinge (1999), Simultaneous observations of energetic ((150 keV) protons upstream of the Earth's bow shock at ACE and Wind, *Geophys. Res. Lett.*, *26*, 169, doi:10.1029/1998GL900288.
Haggerty, D. K., E. C. Roelof, C. W. Smith, N. F. Ness, R. L. Tokar, and R. M. Skoug (2000), Interplanetary magnetic field connection to the L1 Lagrangian orbit during upstream energetic ion events, *J. Geophys. Res.*, *105*, 25123, doi:10.1029/1999JA000346.
Ipavich, F. M., J. T. Gosling, and M. Scholer (1984), Correlation between the He/H ratios in upstream particle events and in the solar wind, *J. Geophys. Res.*, *89*(A3), 1501–1507, doi:10.1029/JA089iA03p01501.
Ipavich, F. M., G. Gloeckler, D. C. Hamilton, L. M. Kistler, and J. T. Gosling (1988), Protons and alpha-particles in field-aligned beams upstream of the bow shock, *Geophys. Res. Lett.*, *15*(10), 1153–1156, doi:10.1029/GL015i010p01153.
Jones, F. C., and D. C. Ellison (1991), The plasma physics of shock acceleration, *Space Sci. Rev.*, *58*, 259–346, doi:10.1007/BF01206003.
Kahler, S. W., E. Hildner, and M. A. I. Van Hollebeke (1978), Prompt solar proton events and coronal mass ejections, *Sol. Phys.*, *57*, 429, doi:10.1007/BF00160116.
Kahler, S. W., N. R. Sheeley Jr., R. A. Howard, D. J. Michels, M. J. Koomen, R. E. McGuire, T. T. von Rosenvinge, and D. V. Reames (1984), Associations between coronal mass ejections and solar energetic proton events, *J. Geophys. Res.*, *89*, 9683, doi:10.1029/JA089iA11p09683.
Kahler, S. W., D. V. Reames, and N. R. Sheeley Jr. (2001), Coronal mass ejections associated with impulsive solar energetic particle events, *Astrophys. J.*, *562*(1), 558–565, doi:10.1086/323847.
Kennel, C. F., F. V. Coroniti, F. L. Scarf, W. A. Livesey, C. T. Russell, and E. J. Smith (1986), A test of Lee's quasi-linear theory of ion acceleration by interplanetary traveling shocks, *J. Geophys. Res.*, *91*, 11,917–11,928, doi:10.1029/JA091iA11p11917.
Kis, A., M. Scholer, B. Klecker, E. Möbius, E. A. Lucek, H. Rème, J. M. Bosqued, L. M. Kistler, and H. Kucharek (2004), Multi-spacecraft observations of diffuse ions upstream of Earth's bow shock, *Geophys. Res. Lett.*, *31*, L20801, doi:10.1029/2004GL020759.
Klecker, B., E. Möbius, and M. A. Popecki (2006), Solar energetic particle charge states: An overview, *Space Sci. Rev.*, *124*(1–4), 289–301, doi:10.1007/s11214-006-9111-0.
Kocharov, G. E. (1983), Energetic particle and gamma-ray generation in the solar matter, in *Proceedings of 18th International Cosmic Ray Conference*, vol. 12, pp. 235–256, Tata Inst. of Fundam. Res., Mumbai, India.
Korreck, K. E., T. H. Zurbuchen, S. T. Lepri, and J. M. Raines (2007), Heating of heavy ions by interplanetary coronal mass ejection driven collisionless shocks, *Astrophys. J.*, *659*(1), 773–779, doi:10.1086/512360.
Kucharek, H., and M. Scholer (1991), Origin of diffuse superthermal ions at quasi-parallel supercritical collisionless shocks, *J. Geophys. Res.*, *96*, 21195, doi:10.1029/91JA02321.
Kucharek, H., and M. Scholer (1995), Injection and acceleration of interstellar pickup ions at the heliospheric termination shock, *J. Geophys. Res.*, *100*, 1745, doi:10.1029/94JA02559.
Kucharek, H., E. Möbius, W. Li, C. J. Farrugia, M. A. Popecki, A. B. Galvin, B. Klecker, M. Hilchenbach, and P. A. Bochsler (2003), On the source and acceleration of energetic He^+: A long-term observation with ACE/SEPICA, *J. Geophys. Res.*, *108*(A10), 8040, doi:10.1029/2003JA009938.
Kucharek, H., E. Möbius, M. Scholer, C. Mouikis, L. Kistler, T. Horbury, A. Balogh, H. Rème, and J. Bosqued (2004), On the origin of field-aligned beams at the quasi-perpendicular bow shock: Multi-spacecraft observations by Cluster, *Ann. Geophys.*, *22*, 2301–2308.
Lario, D., Q. Hu, G. C. Ho, R. B. Decker, E. C. Roelof, and C. W. Smith (2005a), Statistical properties of fast forward transient interplanetary shocks and energetic particle events: ACE observations, in *Connecting Sun and Heliosphere: Proceedings of Solar Wind 11 and SOHO 16*, *Eur. Space Agency Spec. Publ.*, *ESA-SP 592*, 81–86.
Lario, D., R. B. Decker, G. C. Ho, Q. Hu, C. W. Smith, M. I. Desai, and A.-F. Viñas (2005b), The energetic storm particle event on 2003 October 24: A test of diffusive shock acceleration theory, in *The Physics of Collisionless Shocks: 4th Annual International Astrophysics Conference*, edited by G. Li, G. P. Zank, and C. T. Russell, *AIP Conf. Proc.*, *781*, 180–184.
Lee, M. A. (1982), Coupled hydromagnetic wave excitation and ion-acceleration upstream of the Earth's bow shock, *J. Geophys. Res.*, *87*(A7), 5063–5080, doi:10.1029/JA087iA07p05063.
Lee, M. A. (1983), Coupled hydromagnetic wave excitation and ion acceleration at interplanetary traveling shocks, *J. Geophys. Res.*, *88*, 6109–6119, doi:10.1029/JA088iA08p06109.
Leske, R. A., R. A. Mewaldt, A. C. Cummings, E. C. Stone, and T. T. von Rosenvinge (2001), The ionic charge state composition at high energies in large solar energetic particle events in solar cycle 23, *AIP Conf. Proc.*, *598*, 171, doi:10.1063/1.1433996.
Leske, R. A., C. M. S. Cohen, A. C. Cummings, R. A. Mewaldt, E. C. Stone, M. E. Wiedenbeck, and T. T. von Rosenvinge (2005), Ultra-heavy elements above 10 MeV/nucleon in solar energetic particle events, in *Proceedings of the 29th International Cosmic Ray Conference, Pune, India*, vol. 1, edited by B. S. Acharya et al., p. 107, Tata Inst. of Fundam. Res., Mumbai, India.
Li, G., and G. P. Zank (2005), Mixed particle acceleration at CME-driven shocks and flares, *Geophys. Res. Lett.*, *32*(2), L02101, doi:10.1029/2004GL021250.
Li, G., G. P. Zank, and W. K. M. Rice (2003), Energetic particle acceleration and transport at coronal mass ejection-driven shocks, *J. Geophys. Res.*, *108*(A2), 1082, doi:10.1029/2002JA009666.
Li, G., G. P. Zank, and W. K. M. Rice (2005), Acceleration and transport of heavy ions at coronal mass ejection-driven shocks, *J. Geophys. Res.*, *110*(A6), A06104, doi:10.1029/2004JA010600.
Lin, R. P. (1970), The emission and propagation of 40 keV solar flare electrons. I: The relationship of 40 keV electron to energetic proton and relativistic electron emission by the Sun, *Sol. Phys.*, *12*, 266, doi:10.1007/BF00227122.
Luhn, A., B. Klecker, D. Hovestadt, M. Scholer, G. Gloeckler, F. M. Ipavich, C. Y. Fan, and L. A. Fisk (1984), Ionic charge states of N, Ne, Mg, SI and S in solar energetic particle events, *Adv. Space Res.*, *4*(2–3), 161, doi:10.1016/0273-1177(84)90307-7.
Manchester, W. B., IV, T. I. Gombosi, D. L. De Zeeuw, I. V. Sokolov, K. G. Powell, J. Kóta, G. Tóth, and T. H. Zurbuchen (2005), Coronal mass ejection shock and sheath structures relevant to particle acceleration, *Astrophys. J.*, *622*(2), 1225–1239, doi:10.1086/427768.
Mason, G. M., G. Gloeckler, and D. Hovestadt (1984), Temporal variations of nucleonic abundances in solar flare energetic particle events. II - Evidence for large-scale shock acceleration, *Astrophys. J.*, *280*, 902, doi:10.1086/162066.
Mason, G. M., J. E. Mazur, and T. T. von Rosenvinge (1996), Energetic heavy ions observed upstream of the Earth's bow shock by the STEP/EPACT instrument on Wind, *Geophys. Res. Lett.*, *23*, 1231, doi:10.1029/96GL01035.
Mason, G. M., et al. (1998), The Ultra-Low-Energy Isotope Spectrometer (ULEIS) for the ACE spacecraft, *Space Sci. Rev.*, *86*(1–4), 409–448, doi:10.1023/A:1005079930780.
Mason, G. M., J. E. Mazur, and J. R. Dwyer (1999), ^{3}He enhancements in large solar energetic particle events, *Astrophys. J.*, *525*, L133, doi:10.1086/312349.
Mason, G. M., J. E. Mazur, J. R. Dwyer, J. R. Jokipii, R. E. Gold, and S. M. Krimigis (2004), Abundances of heavy and ultraheavy ions in ^{3}He-rich solar flares, *Astrophys. J.*, *606*, 555, doi:10.1086/382864.
Mason, G. M., M. I. Desai, J. E. Mazur, and J. R. Dwyer (2005), Energetic particles accelerated by shocks in the heliosphere: What is the source material?, in *The Physics of Collisionless Shocks*, edited by G. Li, G. P. Zank, and C. T. Russell, *AIP Conf. Proc.*, *781*, 227.
Mason, G. M., M. I. Desai, C. M. S. Cohen, R. A. Mewaldt, E. C. Stone, and J. R. Dwyer (2006), The role of interplanetary scattering in western hemisphere large solar energetic particle events, *Astrophys. J.*, *647*(1), L65–L68, doi:10.1086/507469.
Mason, G. M., R. A. Leske, M. I. Desai, J. R. Dwyer, J. E. Mazur, R. A. Mewaldt, R. E. Gold, and S. M. Krimigis (2008), Abundances and energy spectra of corotating interaction region heavy ions observed during solar cycle 23, *Astrophys. J.*, *678*, 1458–1470, doi:10.1086/533524.
Mazur, J. E., G. M. Mason, M. D. Looper, R. A. Leske, and R. A. Mewaldt (1999), Charge states of solar energetic particles using the geomagnetic cutoff technique: SAMPEX measurements in the 6 November 1997 solar particle event, *Geophys. Res. Lett.*, *26*, 173, doi:10.1029/1998GL900075.
Mewaldt, R. A., et al. (2001), Long-term fluences of energetic particles in the heliosphere, in *Solar and Galactic Composition*, *AIP Conf. Proc.*, *598*, 165, doi:10.1063/1.1433995.
Mewaldt, R. A., C. S. Cohen, and G. M. Mason (2006), The source material for large solar energetic particle events, in *Solar Eruptions and Energetic Particles*, *Geophys. Monogr. Ser.*, vol. 165, pp. 115–126, AGU, Washington, D.C.
Meyer, P., E. N. Parker, and J. A. Simpson (1956), Solar cosmic rays of February, 1956 and their propagation through interplanetary space, *Phys. Rev.*, *104*, 768, doi:10.1103/PhysRev.104.768.

Meziane, K., et al. (2004), Simultaneous observations of field-aligned beams and gyrating ions in the terrestrial foreshock, *J. Geophys. Res.*, *109*, A05107, doi:10.1029/2003JA010374.
Mitchell, D. G., and E. C. Roelof (1983), Dependence of 50-keV upstream ion events at IMP 7 and 8 upon magnetic field bow shock geometry, *J. Geophys. Res.*, *88*, 5623, doi:10.1029/JA088iA07p05623.
Möbius, E., D. Hovestadt, B. Klecker, M. Scholer, F. M. Ipavich, C. W. Carlson, and R. P. Lin (1986), A burst of energetic O+ ions during an upstream particle event, *Geophys. Res. Lett.*, *13*(13), 1372–1375, doi:10.1029/GL013i013p01372.
Möbius, E., et al. (1999), Energy dependence of the ionic charge state distribution during the November 1997 solar energetic particle event, *Geophys. Res. Lett.*, *26*, 145–148, doi:10.1029/1998GL900131.
Möbius, E., et al. (2001), Observations of the spatial and temporal structure of field-aligned beam and gyrating ring distributions at the quasi-perpendicular bow shock with Cluster CIS, *Ann. Geophys.*, *19*, 1411–1420.
Müller-Mellin, R., R. Gomez-Herrero, S. Böttcher, A. Klassen, B. Heber, R. Wimmer-Schweingruber, L. Duvet, and T. R. Sanderson (2007), Upstream events and recurrent CIR-accelerated particle events observed by Stereo/SEPT, paper 0924 presented at 30th International Cosmic Ray Conference, Univ. Nac. Auton. de Mex., Merida, Mexico.
Ng, C. K., D. V. Reames, and A. J. Tylka (2003), Modeling shock-accelerated solar energetic particles coupled to interplanetary Alfvén waves, *Astrophys. J.*, *591*(1), 461–485, doi:10.1086/375293.
Oetliker, M., B. Klecker, D. Hovestadt, G. M. Mason, J. E. Mazur, R. A. Leske, R. A. Mewaldt, J. B. Blake, and M. D. Looper (1997), The ionic charge of solar energetic particles with energies of 0.3–70 MeV per nucleon, *Astrophys. J.*, *477*, 495, doi:10.1086/303679.
Oka, M., T. Terasawa, Y. Saito, and T. Mukai (2005), Field-aligned beam observations at the quasi-perpendicular bow shock: Generation and shock angle dependence, *J. Geophys. Res.*, *110*, A05101, doi:10.1029/2004JA010688.
Paschmann, G., N. Sckopke, I. Papamastorakis, J. R. Asbridge, S. J. Bame, and J. T. Gosling (1981), Characteristics of reflected and diffuse ions upstream from the Earth's bow shock, *J. Geophys. Res.*, *86*(A6), 4355–4364, doi:10.1029/JA086iA06p04355.
Posner, A., N. A. Schwadron, T. H. Zurbuchen, J. U. Kozyra, M. W. Liemohn, and G. Gloeckler (2002), Association of low-charge-state heavy ions up to 200 R_e upstream of the Earth's bow shock with geomagnetic disturbances, *Geophys. Res. Lett.*, *29*(7), 1099, doi:10.1029/2001GL013449.
Reames, D. V. (1988), Bimodal abundances in the energetic particles of solar and interplanetary origin, *Astrophys. J.*, *330*, L71, doi:10.1086/185207.
Reames, D. V. (1999), Particle acceleration at the Sun and in the heliosphere, *Space Sci. Rev.*, *90*, 413, doi:10.1023/A:1005105831781.
Sanderson, T. R., R. Reinhard, and K.-P. Wenzel (1981), The propagation of upstream protons between the Earth's bow shock and ISEE-3, *J. Geophys. Res.*, *86*, 4425, doi:10.1029/JA086iA06p04425.
Sanderson, T. R., R. Reinhard, P. van Ness, and K.-P. Wenzel (1985), Observations of three-dimensional anisotropies of 35- to 1000-keV protons associated with interplanetary shocks, *J. Geophys. Res.*, *90*, 19–27, doi:10.1029/JA090iA01p00019.
Sarris, E. T., S. M. Krimigis, and T. P. Armstrong (1976), Observations of magnetospheric bursts of high energy protons and electrons at 35 RE with IMP 7, *J. Geophys. Res.*, *81*, 2341, doi:10.1029/JA081i013p02341.
Sarris, E. T., S. M. Krimigis, C. O. Bostrom, and T. P. Armstrong (1978), Simultaneous multispacecraft observations of energetic proton bursts inside and outside the magnetosphere, *J. Geophys. Res.*, *83*, 4289, doi:10.1029/JA083iA09p04289.
Sarris, E. T., G. C. Anagnostopoulos, and S. M. Krimigis (1987), Simultaneous measurements of energetic ($\geq$50 keV) and electron ($\geq$220 keV) activity upstream of Earth's bow shock and inside the plasma sheet: Magnetospheric source of the November 3 and December 3, 1977 upstream events, *J. Geophys. Res.*, *92*, 12083, doi:10.1029/JA092iA11p12083.
Scholer, M. (1985), Diffusive acceleration, in *Collisionless Shocks in the Heliosphere: Reviews of Current Research*, *Geophys. Monogr. Ser.*, vol. 35, edited by B. T. Tsurutani and R. G. Stone, pp. 287–301, AGU, Washington, D.C.
Scholer, M., G. Gloeckler, F. M. Ipavich, D. Hovestadt, and B. Klecker (1979), Pitch angle distributions of energetic protons near the Earth's bow shock, *Geophys. Res. Lett.*, *6*, 707, doi:10.1029/GL006i009p00707.
Scholer, M., F. M. Ipavich, G. Gloecker, and D. Hovestadt (1981), Simultaneous observations of energetic protons close to the bow shock and far upstream, *J. Geophys.*, *49*, 186.
Scholer, M., H. Kucharek, and K.-H. Trattner (1999), Injection and acceleration of H+ and He2+ at Earth's bow shock, *Ann. Geophys.*, *17*, 583–594.
Schwartz, S. (2006), Shocks: Commonalities in solar-terrestrial chains, *Space Sci. Rev.*, *124*(1–4), doi:10.1007/s11214-006-9093-y.
Sheldon, R. B., J. Chen, and T. A. Fritz (2003), Comment on "Origins of energetic ions in the cusp" by K. J. Trattner et al., *J. Geophys. Res.*, *108*(A7), 1302, doi:10.1029/2002JA009575.
Sonnerup, B. U. Ö. (1969), Acceleration of particles reflected at a shock front, *J. Geophys. Res.*, *74*, 1301–1304, doi:10.1029/JA074i005p01301.
Stone, E. C., A. M. Fransden, R. A. Mewaldt, E. R. Christian, D. Margoiles, J. F. Ormes, and F. Snow (1998a), The Advanced Composition Explorer, *Space Sci. Rev.*, *86*(1/4), 1–22, doi:10.1023/A:1005082526237.
Stone, E. C., et al. (1998b), The Cosmic Ray Isotope Spectrometer for the Advanced Composition Explorer, *Space Sci. Rev.*, *86*(1/4), 285–356, doi:10.1023/A:1005075813033.
Stone, E. C., A. C. Cummings, F. B. McDonald, B. C. Heikkilla, N. Lal, and W. R. Webber (2005), Voyager 1 explores the termination shock region and the heliosheath beyond, *Science*, *309*, 2017–2019, doi:10.1126/science.1117684.
Tanaka, M., C. C. Goodrich, D. Winske, and K. Papadopoulos (1983), A source of the backstreaming ion beams in the foreshock region, *J. Geophys. Res.*, *88*, 3046–3054, doi:10.1029/JA088iA04p03046.
Trattner, K.-J., E. Möbius, M. Scholer, B. Klecker, M. Hilchenbach, and H. Lühr (1994), Statistical analysis of diffuse ion events upstream of the Earth's bow shock, *J. Geophys. Res.*, *99*, 13389, doi:10.1029/94JA00576.
Trattner, K. J., S. A. Fuselier, W. K. Peterson, S.-W. Chang, R. Friedel, and M. R. Aellig (2003), Reply to comment on "Origins of energetic ions in the cusp" by R. Sheldon, J. Chen, and T. A. Fritz, *J. Geophys. Res.*, *108*(A7), 1303, doi:10.1029/2002JA009781.
Tylka, A. J., and M. A. Lee (2006), A model for spectral and compositional variability at high energies in large, gradual solar particle events, *Astrophys. J.*, *646*(2), 1319–1334, doi:10.1086/505106.
Tylka, A. J., C. M. S. Cohen, W. F. Dietrich, M. A. Lee, C. G. Maclennan, R. A. Mewaldt, C. K. Ng, and D. V. Reames (2005), Shock geometry, seed populations, and the origin of variable elemental composition at high energies in large gradual solar particle events, *Astrophys. J.*, *625*(1), 474–495, doi:10.1086/429384.
von Steiger, R., N. A. Schwadron, L. A. Fisk, J. Geiss, G. Gloeckler, S. Hefti, B. Wilken, R. F. Wimmer-Schweingruber, and T. H. Zurbuchen (2000), Composition of quasi-stationary solar wind flows from Ulysses/Solar Wind Ion Composition Spectrometer, *J. Geophys. Res.*, *105*, 27217, doi:10.1029/1999JA000358.
Wang, Y.-M., M. Pick, and G. M. Mason (2006), Coronal holes, jets, and the origin of ^{3}He-rich particle events, *Astrophys. J.*, *639*(1), 495–509, doi:10.1086/499355.
Wild, J. P., S. F. Smerd, and A. A. Weiss (1963), Solar bursts, *Annu. Rev. Astron. Astrophys.*, *1*, 291, doi:10.1146/annurev.aa.01.090163.001451.
Wilson, L. B., III, C. Cattell, P. J. Kellog, K. Goetz, K. Kersten, L. Hanson, R. MacGregor, and J. C. Kasper (2007), Waves in interplanetary shocks: A Wind/WAVES study, *Phys. Rev. Lett.*, *99*(4), 041101, doi:10.1103/PhysRevLett.99.041101.
Winske, D., and M. M. Leroy (1984), Diffuse ions produced by electromagnetic ion beam instabilities, *J. Geophys. Res.*, *89*, 2673–2688, doi:10.1029/JA089iA05p02673.
Zank, G. P., W. K. M. Rice, and C. C. Wu (2000), Particle acceleration and coronal mass ejection driven shocks: A theoretical model, *J. Geophys. Res.*, *105*(A11), 25,079–25,096, doi:10.1029/1999JA000455.
Zank, G. P., G. Li, V. Florinski, Q. Hu, D. Lario, and C. W. Smith (2006), Particle acceleration at perpendicular shock waves: Model and observations, *J. Geophys. Res.*, *111*, A06108, doi:10.1029/2005JA011524.

D. Burgess, Astronomy Unit, Queen Mary, University of London, Mile End Road, London E1 4NS, UK.
M. I. Desai, Southwest Research Institute, 6220 Culebra Road, San Antonio, TX 78238, USA. (mdesai@swri.edu)